Polymer Chemistry

Accepted Manuscript

This is an *Accepted Manuscript*, which has been through the Royal Society of Chemistry peer review process and has been accepted for publication.

Accepted Manuscripts are published online shortly after acceptance, before technical editing, formatting and proof reading. Using this free service, authors can make their results available to the community, in citable form, before we publish the edited article. We will replace this *Accepted Manuscript* with the edited and formatted *Advance Article* as soon as it is available.

You can find more information about *Accepted Manuscripts* in the Information for Authors.

Please note that technical editing may introduce minor changes to the text and/or graphics, which may alter content. The journal's standard Terms & Conditions and the Ethical guidelines still apply. In no event shall the Royal Society of Chemistry be held responsible for any errors or omissions in this *Accepted Manuscript* or any consequences arising from the use of any information it contains.

ROYAL SOCIETY OF CHEMISTRY

www.rsc.org/polymers

Electrochemical synthesis of electrochromic polycarbazole films from *N*-phenyl-3,6-bis(*N*-carbazolyl)carbazoles†

Sheng-Huei Hsiao* and Shu-Wei Lin

Department of Chemical Engineering and Biotechnology, National Taipei University of Technology, Taipei 10608, Taiwan. E-mail: shhsiao@ntut.edu.tw

† Electronic supplementary information (ESI) available: See DOI: 10.1039/….

(Abstract)

Two compounds with a tri-carbazole (3Cz) structure, namely 3,6-di(carbazol-9-yl)-*N*-(4-nitrophenyl)carbazole (NO_2-3Cz) and 3,6-di(carbazol-9-yl)-*N*-(4-aminophenyl)carbazole (NH_2-3Cz), were synthesized and electropolymerized into robust polymer films on the electrode surface in an electrolyte solution via the oxidative coupling reactions. The electro-generated polymer films exhibited reversible electrochemical oxidation processes, with a significant electrochromic behaviour. The colour of P(NO_2-3Cz) film changed from pale yellow neutral state to yellow-green as a radical cation and then to blue when fully oxidized. Upon oxidation, the colour of P(NH_2-3Cz) film changed from colourless to pale green and finally to blue. Furthermore, we also synthesized and characterized some *N*-phenylcarbazoles with different substituents on the phenyl group. Based on a comparative study, the possible electropolymerization mechanisms of the NO_2-3Cz and NH_2-3Cz monomers are suggested; that of the former is through carbazole-carbazole coupling, and the latter is through both carbazole-carbazole and NH_2-carbazole couplings.

Introduction

Electrochromism (EC) refers to the reversible electromagnetic absorbance/transmittance and color change resulting from the oxidation or the reduction of the material in response to an externally applied potential by electrochemical means.[1] This functionality is of great interest for a wide range of applications, including smart window,[2] memory elements,[3] electrochromic display,[4] and camouflage materials.[5] Recent high-profile commercialization of electrochromic materials includes the Boeing 787 Dreamliner windows manufactured by Gentex.[6] The most studied electrochromic materials including transition metal oxides,[7] inorganic coordination complexes,[8] small organic molecules,[9] and conjugated polymers.[10] Among the available electrochromic materials, π-conjugated polymers have attracted tremendous attention because of combined several advantages such as mechanical flexibility, high optical contrast ratios, long-term redox stability and easy color tuning through structural control.[11] In addition, triarylamine-containing condensation-type high performance polymers such as aromatic

polyamides and polyimides have been developed as a new family of electrochromic materials.[12−14]

Polymers containing carbazole moieties in the main chain or side chain have attracted much attention because of their unique properties, which allow various optoelectronic applications such as photoconductive, electroluminescent, electrochromic, and photorefractive materials.[15] Carbazole-based derivatives simultaneously possess carrier-transport properties and sufficiently high triplet energy levels, and therefore, oligocarbazoles or carbazole dendrons via 3(6), 9-linkages have been used as effective host materials for phosphorescent metal complexes.[16] Carbazole can be substituted or polymerized either at the 3- and 6- positions or 2- and 7- positions and a wide variety of alkyl and aryl chains can be added on the nitrogen atom without altering the planar conformation of the resulting polymers. Using different synthetic strategies and substitution patterns, the physic-chemical properties of poly(3,6-carbazole)s and poly(2,7-carbazole)s can be fine-tuned, leading to high performance materials for a number electronic applications.[17] On the other hand, the electrochemical oxidation of carbazole and *N*-substituted derivatives was first studied by Ambrose and Nelson.[18(a)] They further studied systematically 76 ring-substituted carbazoles about their substituent effects using electrochemical and spectroscopic techniques.[18(b)] For the *N*-phenylcarbazoles (NPCs) with both the 3 and 6 carbazole ring positions unprotected, these compounds underwent an initial one-electron oxidation to generate a very reactive cation radical; two of these then coupled at the 3 positions to yield a *N,N*'-diphenyl-3,3'-bicarbazyl. This carbazole oxidative dimerization reaction has been employed efficiently to fabricate electroactive polymeric films for potential applications in electronic and optoelectronic devices.[19] Compared with the chemical routes, electrochemical polymerization has several advantages in the syntheses of conducting polymer films, such as one-step polymer film formation with good mechanical properties on the electrode.[20] This is not only enlarges the scope of candidate polymers, but also omits the procedure of the film casting.

In this work, we have synthesized a series of NPCs (Scheme 1) in which the *para* position of the *N*-phenyl group has been substituted with various groups such as cyano, carboxyl, nitro, and amino groups. Their electrochemistry and electropolymerization and the substituent effect on the redox properties of carbazoles were investigated. We found that the oxidized forms of NPC, CN-NPC, COOH-NPC, and NO_2-NPC underwent dimerization to the corresponding biscarbazoles, whereas NH_2-NPC could undergo electrochemical polymerization to form polymer thin film on the electrode surface via the electropolymerization mechanism likely similar to that of polyaniline. Then two *N*-phenyl-3,6-bis(*N*-carbazolyl)carbazoles, i.e., NO_2-3Cz and NH_2-3Cz as shown in Scheme 2, were prepared and the P(NO_2-3Cz) and P(NH_2-3Cz) films were prepared directly on the electrode surface via electrochemical oxidative coupling of carbazole-carbazole and amine-carbazole. The electrochromic properties of the resulting polycarbazole films were evaluated by the spectroelectrochemical and electrochromic switching studies.

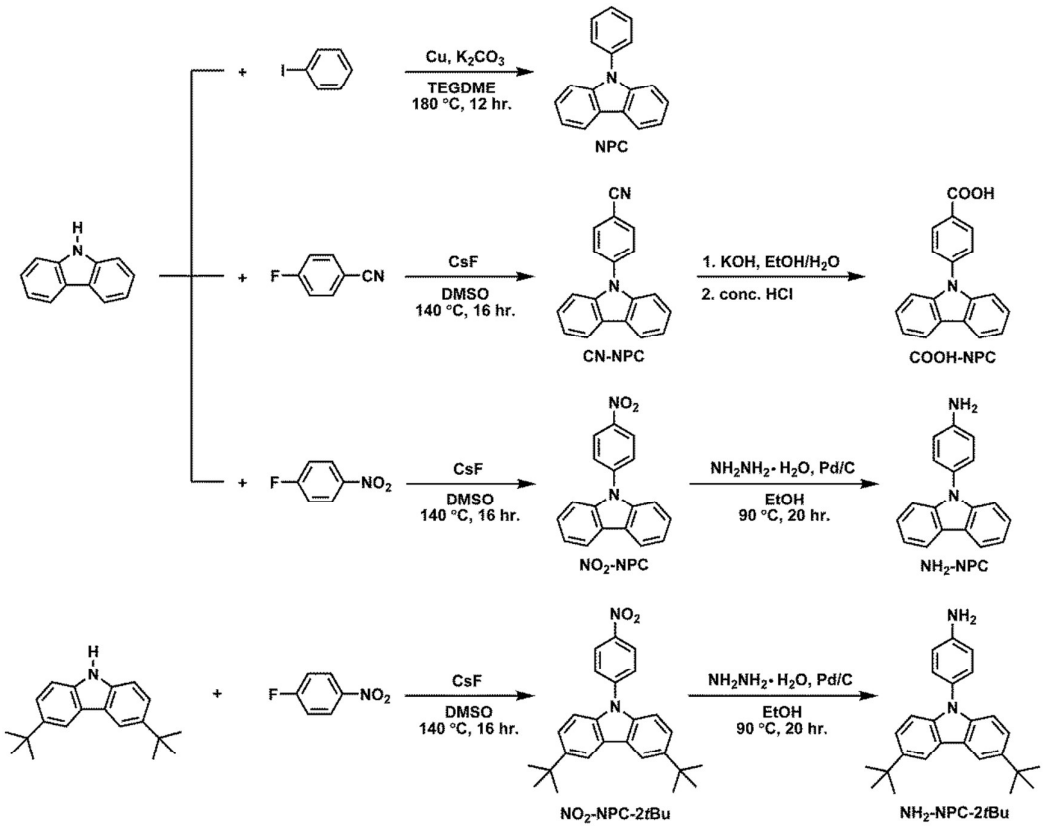

Scheme 1 Synthetic routes to *N*-phenylcarbazoles.

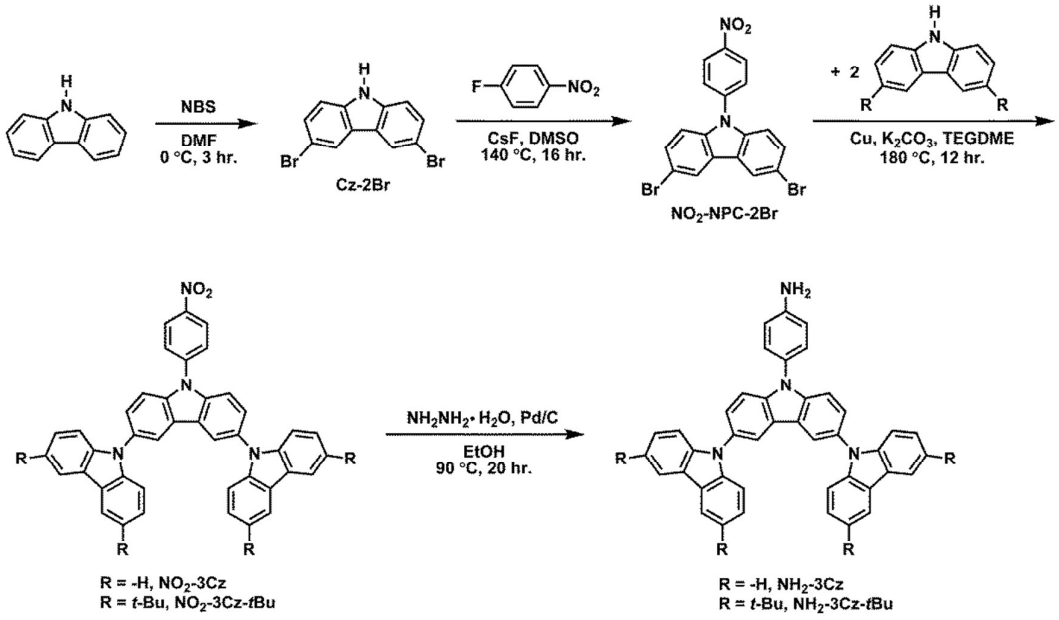

Scheme 2 Synthetic routes to 3,6-bis(*N*-carbazolyl)-*N*-phenylcarbazoles.

Experimental section

Materials and instrumentation

N-Phenylcarbazole (NPC), *N*-(4-nitrophenyl)carbazole (NO_2-NPC), *N*-(4-aminophenyl)carbazole (NH_2-NPC), 3,6-di-*tert*-butyl-9-(4-nitrophenyl)carbazole (NO_2-NPC-2*t*Bu) and 3,6-di-*tert*-butyl-9-(4-aminophenyl)carbazole (NH_2-NPC-2*t*Bu) were synthesized according to literature methods.[21] *N*-(4-carboxyphenyl)carbazole (COOH-NPC) was synthesized by the cesium fluoride (CsF)-mediated *N*-arylation reaction of carbazole with *p*-fluorobenzonitrile, followed by the alkaline hydrolysis of the intermediate nitrile compound *N*-(4-cyanophenyl)carbazole (CN-NPC). The synthetic route and chemical structures of the *N*-phenylcarbazole derivatives are illustrated in Scheme 1. The functionalities of all the synthesized compounds were confirmed by the IR analysis shown in Fig. S1†. The synthetic details and electrochemical properties (Fig. S2†) of model compounds 3,6-di(3,6-di-*tert*-butylcarbazole-9-yl)-*N*-(4-nitrophenyl)carbazole (NO_2-3Cz-*t*Bu) and 3,6-Di(3,6-di-*tert*-butylcarbazole-9-yl)-*N*-(4-aminophenyl)carbazole (NH_2-3Cz-*t*Bu) are included in the ESI†. All other reagents and solvents were used as received from commercial sources.

Infrared (IR) spectra were recorded on a Horiba FT-720 FT-IR spectrometer. ^{1}H and ^{13}C NMR spectra were measured on a Bruker Avance III HD-600 MHz NMR spectrometer with tetramethylsilane (TMS) as an internal standard. Electrochemical measurements were performed with a CH Instruments 750A electrochemical analyzer. The polymers were electropolymerized from 5 x 10^{-4} M monomers in 0.1 M Bu_4NClO_4/dichloromethane solution via repetitive cycling at a scan rate of 50 mV s^{-1}. Thin films on ITO-glass obtained by two and five cycles between 0 V and 1.5 V at a scan rate of 50 mV s^{-1} were used for UV-Visible absorption measurements and spectroelectrochemistry studies, respectively. Voltammograms are presented with the positive potential pointing to the left and with increasing anodic currents pointing downwards. Cyclic voltammetry (CV) was conducted with the use of a three-electrode cell in which ITO (polymer films area about 0.8 cm x 1.25 cm) was used as a working electrode. A platinum wire used as an auxiliary electrode. All cell potentials were taken with the use of a home-made Ag/AgCl, KCl (sat.) reference electrode. Ferrocene was used as an external reference for calibration (+0.48 V vs. Ag/AgCl). Spectroelectrochemistry analyses were carried out with an electrolytic cell, which was composed of a 1 cm cuvette, ITO as a working electrode, a platinum wire as an auxiliary electrode, and a Ag/AgCl reference electrode. Absorption spectra in the spectroelectrochemical experiments were measured with an Agilent 8453 UV-Visible diode array spectrophotometer. Colorimetric data of the electrochromic films were measured on an Admesy Brontes colorimeter.

Monomer synthesis

3,6-Di(carbazol-9-yl)-*N*-(4-nitrophenyl)carbazole (NO_2-3Cz). A mixture of 3,6-dibromo-*N*-(4-nitrophenyl)carbazole (0.03 mol, 13.38 g), carbazole (0.063 mol, 10.53 g), copper powder (0.063 mol, 4 g), potassium carbonate (0.065 mol, 8.98 g) and triethyleneglycol dimethyl ether (TEGDME) (35 mL) was stirred under nitrogen atmosphere at 180 °C for 12 h. The reaction mixture was poured into excess of methanol to precipitate the product. The yellow precipitate was collected by filtration and washed thoroughly by methanol. The crude product was filtered and re-precipitated three times from the DMF/methanol solvent pair to afford 11.69 g of yellow powder. FT-IR (KBr) (Fig. S3†): 1500, 1322 cm^{-1} ($-NO_2$ stretch). ^1H NMR (600 MHz, $CDCl_3$, δ, ppm) (Fig. S4†): 7.27 (t, J = 6.0 Hz, 4H, H_b), 7.38 (m, 8H, $H_c + H_d$), 7.64 (d, J = 8.4 Hz, 2H, H_e), 7.70 (d, J = 8.4 Hz, 2H, H_f), 7.93 (d, J = 8.4 Hz, 2H, H_h), 8.14 (d, J = 7.8 Hz, 4H, H_a), 8.27 (s, 2H, H_g), 8.56 (d, J = 8.4 Hz, 2H, H_i). ^{13}C NMR (150 MHz, $CDCl_3$, δ, ppm) (Fig. S5†): 109.56 (C^5), 111.15 (C^9), 119.91 (C^3), 119.96 (C^{12}), 120.38 (C^2), 123.28 (C^1), 124.83 (C^{11}), 125.84 (C^{15}), 125.98 (C^4), 126.70 (C^8), 127.06 (C^{14}), 130.52 (C^{13}), 131.57 (C^7), 139.63 (C^{10}), 141.60 (C^6), 146.49 (C^{16}).

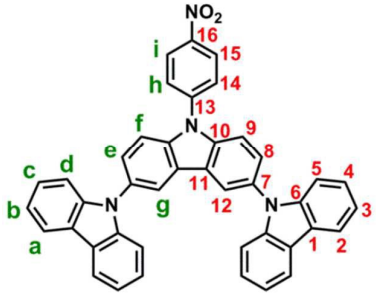

3,6-Di(carbazol-9-yl)-*N*-(4-aminophenyl)carbazole (NH_2-3Cz). In the 1000-mL three-neck round-bottomed flask equipped with a stirring bar, 6.19 g (0.01 mol) of the nitro compound NO_2-3Cz, and 0.05 g of 10 % Pd/C were dissolved/suspended in 600 mL ethanol. The suspension solution was heated to reflux under nitrogen atmosphere, and 1.3 mL of hydrazine monohydrate was added to the reaction mixture. After a further 20 h of reflux, the solution was filtered to remove Pd/C, and the filtrate was cooled under a nitrogen flow to precipitate colorless powder. The product was collected by filtration and dried in vacuo at 80 °C to give 5.06 g of NH_2-3Cz as white fine powder in 86 % yield. FT-IR (KBr) (Fig. S3†): 3472, 3373 cm^{-1} ($-NH_2$ stretch). ^1H NMR (600 MHz, $CDCl_3$, δ, ppm) (Fig. S6†): 3.83 (s, 2H, $-NH_2$), 6.85 (d, J = 8.4 Hz, 2H, H_i), 7.26 (m, 4H, H_b), 7.37 (m, 8H, $H_c + H_d$), 7.39 (d, J = 8.4 Hz, 2H, H_h), 7.54 (m, 4H, $H_f + H_e$), 8.13 (d, J = 7.2 Hz, 2H, H_a), 8.23 (s, 2H, H_g). ^{13}C NMR (150 MHz, $CDCl_3$, δ, ppm) (Fig. S7†): 109.74 (C^5), 111.32 (C^9), 116.01 (C^{15}), 119.63 ($C^3 + C^{12}$), 120.26 (C^2), 123.12 (C^1), 123.53 (C^{11}), 125.86 (C^4), 126.07 (C^8), 127.31 (C^{12}), 128.51 (C^{14}), 129.91 (C^7), 141.35 (C^{10}), 141.86 (C^6), 146.60 (C^{16}).

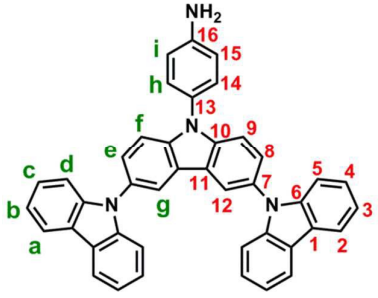

Electrochemical polymerization

Electrochemical polymerization was performed with a CH Instruments 750A electrochemical analyzer. The polymers were synthesized from 5 x 10^{-4} M monomers in 0.1 M Bu_4NClO_4/dichloromethane (CH_2Cl_2) or acetonitrile (MeCN) solution via cyclic voltammetry repetitive cycling at a scan rate of 50 mV s^{-1} for ten cycles. The polymer was deposited onto the surface of the working electrode (ITO/glass surface, polymer film area about 0.8 cm × 1.25 cm), and the film was rinsed with plenty of acetone for the removal of un-reacted monomer, inorganic salts and other organic impurities formed during the process.

Fabrication of electrochromic devices

Electrochromic polymer films were electrodeposited on the ITO-coated glass substrate by the electropolymerization method described above. A gel electrolyte based on poly(methyl methacrylate) (PMMA) (Mw: 120000) and $LiClO_4$ was plasticized with propylene carbonate to form a highly transparent and conductive gel. PMMA (1 g) was dissolved in dry MeCN (4 mL), and $LiClO_4$ (0.1 g) was added to the polymer solution as supporting electrolyte. Then propylene carbonate (1.5 g) was added as a plasticizer. The mixture was then gently heated until gelation. The gel electrolyte was spread on the polymer-coated side of the electrode, and the electrodes were sandwiched. Finally, an epoxy resin was used to seal the device.

Results and discussion

Monomer synthesis

3,6-Bis(*N*-carbazolyl)-*N*-phenylcarbazoles was synthesized starting from carbazole by a four-step reaction sequence as shown in Scheme 2. Cz-2Br was synthesized by bromination of carbazole with *N*-bromosuccinimide (NBS). Nucleophilic fluoro-displacement reaction of *p*-fluorobenzonitrile with Cz-2Br in the presence of cesium fluoride (CsF) resulted in NO_2-NPC-2Br,[22] which was subsequently condensed with carbazole and 3,6-di-*tert*-butylcarbazole, respectively, to NO_2-3Cz and NO_2-3Cz-*t*Bu via the Ullmann reaction. The amino compounds NH_2-3Cz and NH_2-3Cz-*t*Bu were prepared by the hydrazine Pd/C-catalyzed reduction of their precursor nitro compounds. FT-IR and NMR spectroscopic techniques were used to identify structures of the synthesized compounds. The FT-IR spectra of NO_2-3Cz and NO_2-3Cz-*t*Bu give two characteristic bands at around 1500 and 1322−1337 cm^{-1} ascribed to the nitro groups (Fig. S3†). The N−H stretching absorptions of NH_2-3Cz and NH_2-3Cz-*t*Bu occur at

about 3472 and 3373 cm^{-1}. NO_2-3Cz-*t*Bu and NH_2-3Cz-*t*Bu showed an additional aliphatic C−H stretching absorption around 2955−2863 cm^{-1} due to the presence of *tert*-butyl groups. The ^1H, ^{13}C and two-dimensional (2-D) NMR spectra of NO_2-3Cz and NH_2-3Cz are compiled in Figs. S4 to S7†. The ^1H NMR spectra confirm that the nitro group have been completely transformed into amino groups by the high field shift of aromatic protons H_h and H_i and the resonance signals at around 3.84 ppm corresponding to the amino protons. Assignments of each carbon and proton assisted by the 2-D NMR spectra are also indicated in these spectra, and they are in good agreement with their proposed molecular structures.

Electrochemical properties

N-Phenylcarbazoles

Fig. 1(a) shows the repetitive cyclic voltammetry (CV) diagrams of 5 x 10^{-4} M of NO_2-NPC in 0.1 M Bu_4NClO_4/MeCN solution at a potential scan rate of 50 mV s^{-1}. These four NPC derivatives exhibit a similar CV behavior. For the first positive scan, a sharp oxidation peak at E_{pa} = 1.37−1.53 V is observed. In the reverse scan, two reduction peaks are observed. In the second scan, a new oxidation wave at E_{pa} = 1.09−1.20 V appears, which indicates that the carbazole radical cations are involved in very fast electrochemical reactions that produce a carbazole dimer via the ring-ring coupling reaction between the carbazole units [Scheme 3(a)].[18] In the continuous scans, the new oxidation wave gradually grows; however, no significant increase in redox wave current density is observed. The biscarbazoles seem to be the major products during the oxidation processes of these NPCs, indicating they are stable in the oxidized states. No polymer films grow up on the electrode surface. Similar results were observed for other NPCs such as NPC, CN-NPC, and COOH-NPC (See Fig. S8†). The results are similar to those found for other NPC analogs reported in literature.[23] The CV result of NH_2-NPC is completely different [Fig. 1(b)]. In the first scan, two oxidation peaks at 1.00 V and 1.36 V are observed, which may be attributed to the oxidation of the aromatic primary amino group (aniline-like) and the carbazole unit, respectively. As the CV scan continued, two new oxidation peaks at E_{pa} = +0.84 V and +1.18 V gradually grew and the redox wave current intensities increased. We also found that a polymer film deposited on the electrode surface (as can be seen in the inset of Fig. 1(b). We propose that the NH_2−carbazole and carbazole−carbazole oxidative coupling reactions simultaneously during the CV scanning. A possible reaction path is suggested in Scheme 3(b). The polymer films are insoluble in polar organic solvents like *N*-methyl-2-pyrrolidine (NMP) and even in concentrated sulfuric acid, but the film can be removed from the ITO-glass surface after immersing in NMP or concentrated sulfuric acid for a certain period of time. This insolubility of the polymer film may be caused by the fact that crosslinking reactions or tight packing of the polymer chains occurred during the electropolymerization process.

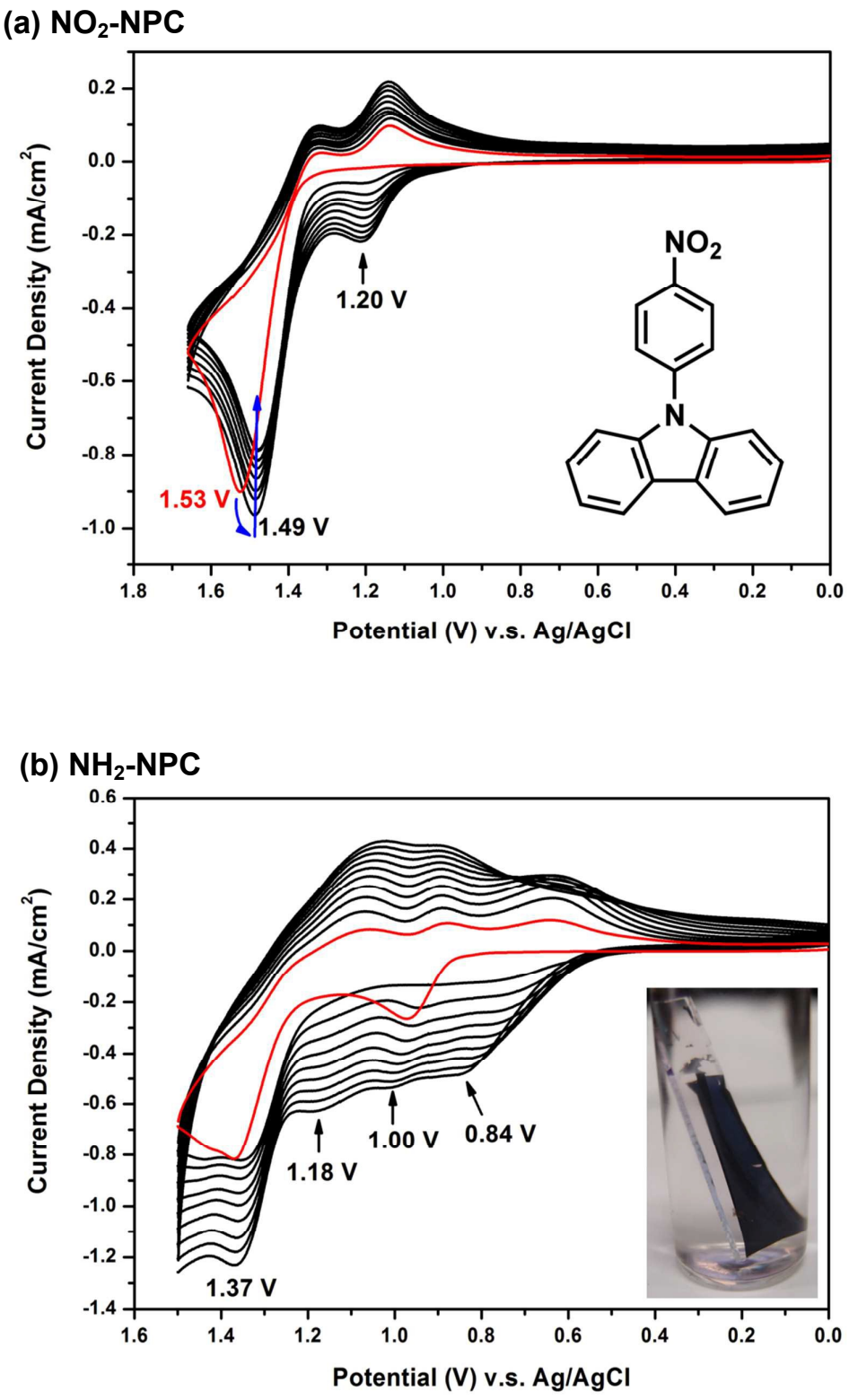

Fig. 1 Repetitive cyclic voltammograms of 5 x 10^{-4} M (a) NO_2-NPC and (b) NH_2-NPC in 0.1 M Bu_4NClO_4/MeCN solution at a scan rate of 50 mV s^{-1}. The inset in (b) displays the escaped polymer film from the ITO glass surface by immersing the film-coated ITO glass in conc. H_2SO_4.

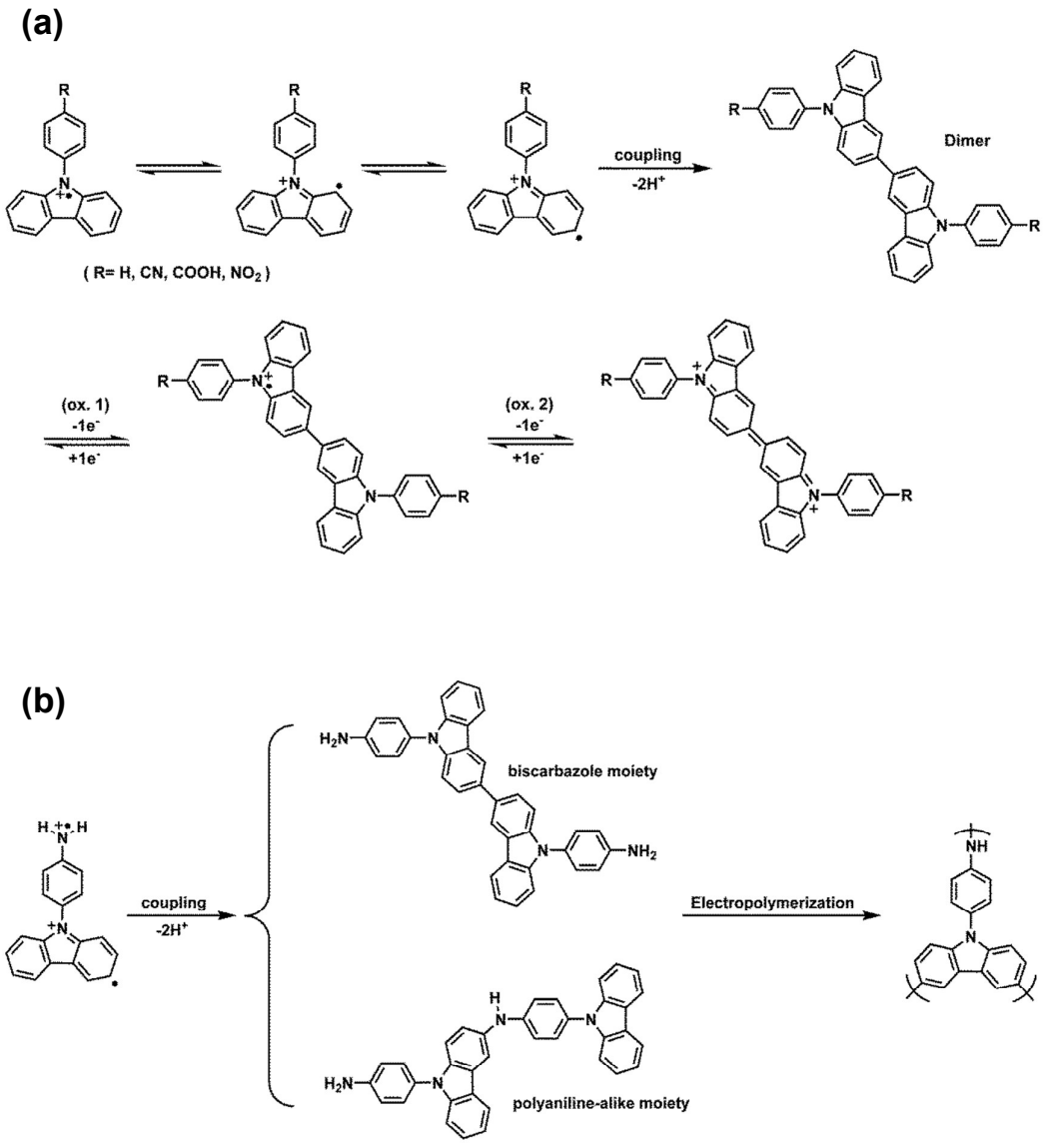

Scheme 3 (a) Electrochemical dimerization of NPCs (R = -H, -CN, -COOH, -NO_2) and subsequent oxidation of the resulting biscarbazoles. (b) Electro-coupling and polymerization of NH_2-NPC.

***N*-Phenyl-3,6-bis(*N*-carbazolyl)carbazoles**

Fig. 2(a) presents the first and second CV scans of 5 x 10^{-4} M NO_2-3Cz in 0.1 M Bu_4NClO_4/CH_2Cl_2 via repetitive cycling at a potential scan rate of 50 mV s^{-1}. In the first scan, only one oxidation peak at 1.46 V is observed, which can be attributed to the oxidation of carbazole. A new oxidation peak appears at about 1.10 V during the second scan, similar to that observed in most NPCs discussed earlier. The carbazole coupling reactions occurring in NO_2-3Cz leads to polymerization. A possible polycarbazole structure may develop as that shown in Scheme 4(a). Thus, as the CV scan continued, the redox wave current densities increased and an obvious polymer film formed on the electrode surface [Fig. 2(b)]. The CV result of NH_2-3Cz is similar to that of NH_2-NPC. Fig. 3(a) displays the first two consecutive CV scans of NH_2-3Cz. In the first scan, this compound displayed two oxidation peaks at 0.98 V and 1.30 V, which is attributed to the oxidation of the aniline-like structure and the carbazole unit, respectively. In the second scan, two new oxidation peaks appeared at 0.79 V and 1.10 V. It is known that biscarbazole unit oxidized at a lower potential than the parent carbazole unit. Thus, we attribute the new oxidation wave at 1.10 V to the biscarbazole unit oxidation and that at 0.79 V to polyaniline-alike unit oxidation [Scheme 4(b)]. After several CV cycles, individual oxidation peak emerged to one broad peak, and the increase in the redox wave current densities implied that the amount of conducting polymers deposited on the electrode was increasing [Fig. 3(b)]. The polymer with polyaniline-alike and biscarbazole units was successfully electrodeposited onto the ITO-glass electrode surface. The lower oxidation potential of NH_2-3Cz compared to NO_2-3Cz can be explained by the electron-donating effect of the amino group.

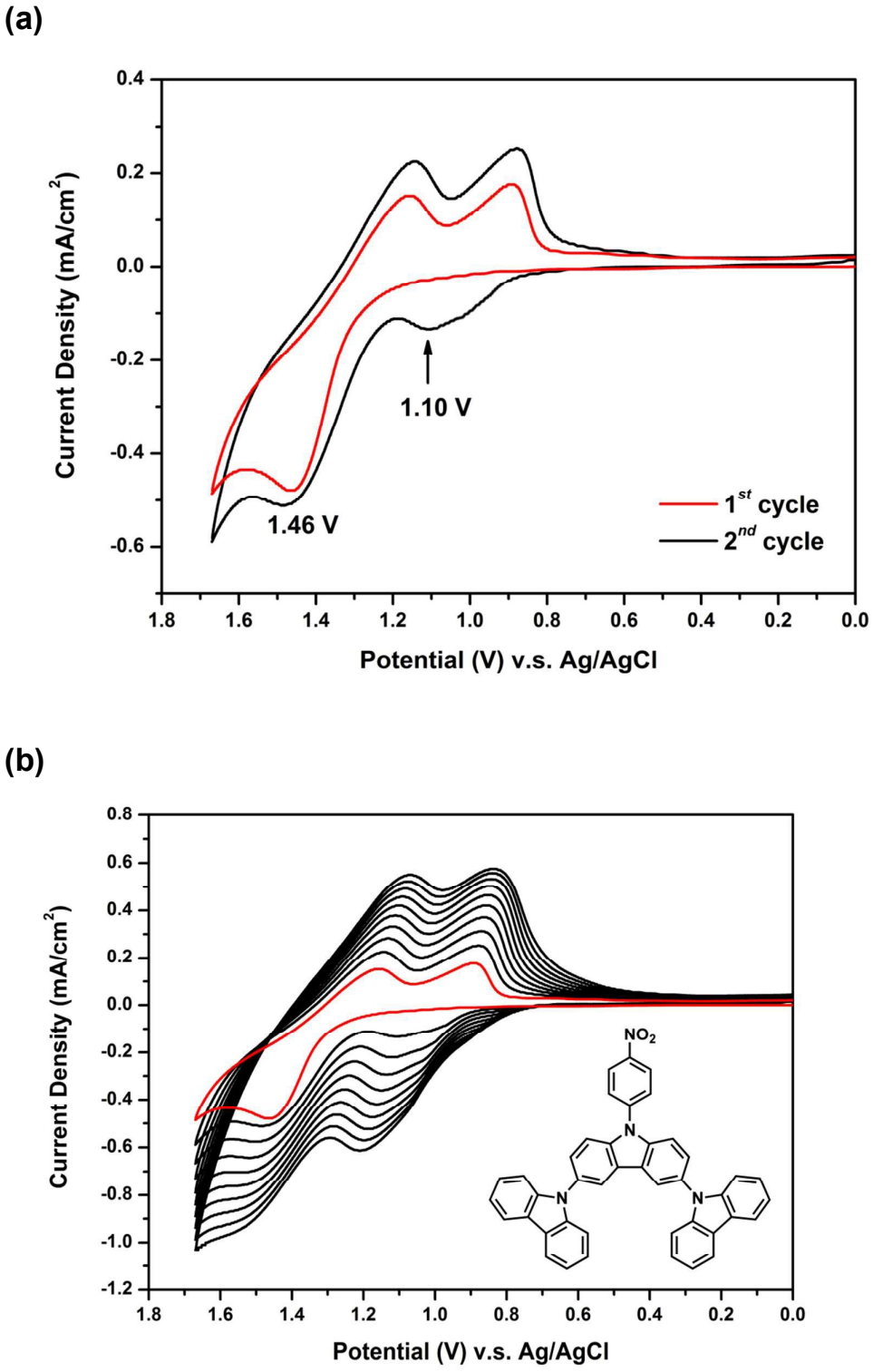

Fig. 2 Cyclic voltammograms and repeated potential scanning of 5 x 10^{-4} M NO_2-3Cz in 0.1 M Bu_4NClO_4/CH_2Cl_2 at a scan rate of 50 mV s^{-1}.

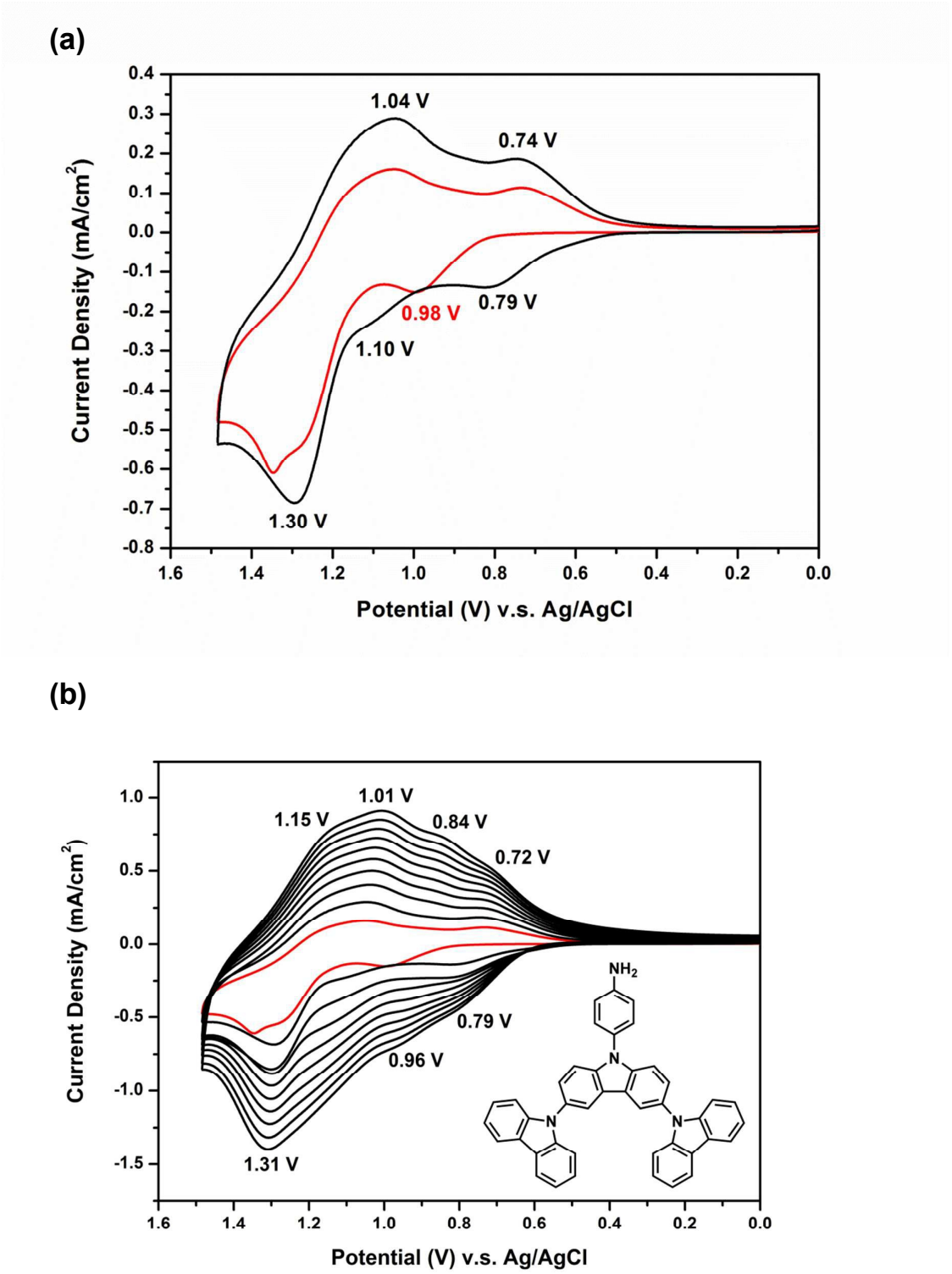

Fig. 3 Cyclic voltammograms and repeated potential scanning of 5 x 10^{-4} M NH_2-3Cz in 0.1 M Bu_4NClO_4/MeCN at a scan rate of 50 mV s^{-1}.

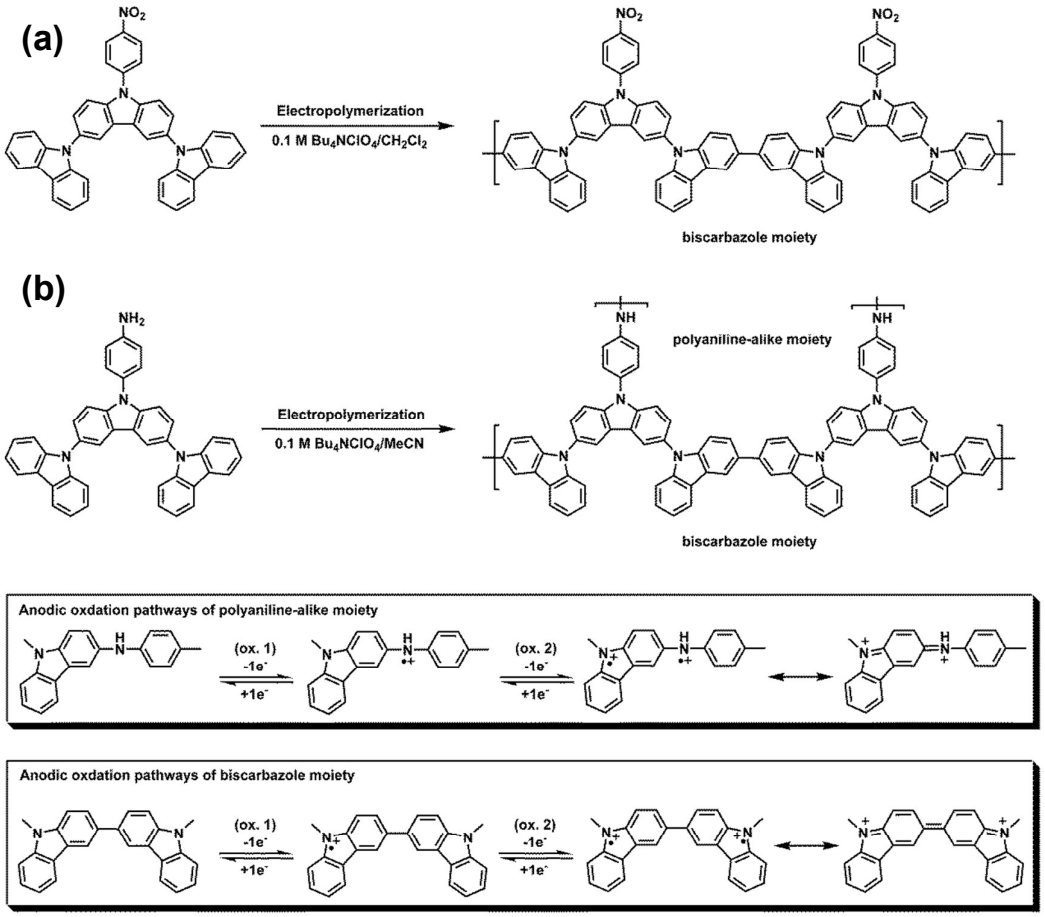

Scheme 4 Electropolymerization of NO_2-3Cz and NH_2-3Cz, together with proposed anodic oxidation pathways of polyaniline-alike moiety and biscarbazole moiety.

Optical and electrochemical properties of the polymer films

The representative UV-vis absorption spectra of monomers NO_2-3Cz and NH_2-3Cz in CH_2Cl_2 and the polymer films of P(NO_2-3Cz) and P(NH_2-3Cz) in solid state on an ITO electrode are shown in Fig. 4. The spectra of the monomers show absorption bands with maximum peaks at 293 nm and absorption onsets at 458 and 365 nm, respectively. The polymer films of P(NO_2-3Cz) and P(NH_2-3Cz) show absorption maxima at 305 and 304 nm, respectively, and the wavelength at absorption edge of the former is much longer than that of the latter possibly due to the charge-transfer complexing effect. The red-shift of absorption maximum and onset of the P(NH_2-3Cz) film compared to the NH_2-3Cz monomer implies an extended π-conjugation length.

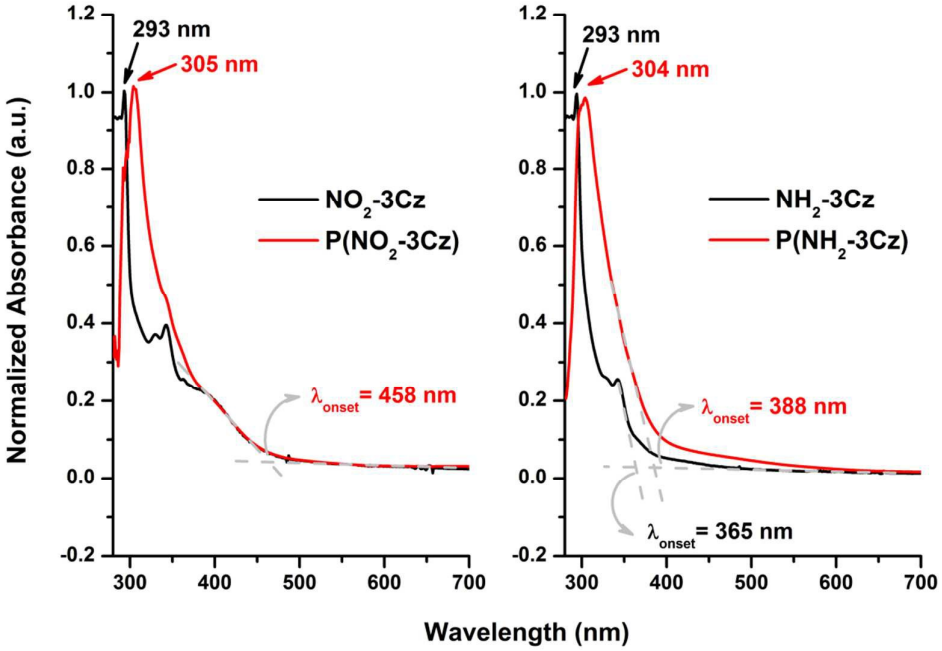

Fig. 4 UV-vis absorption spectra of NO_2-3Cz and NH_2-3Cz in CH_2Cl_2 and the P(NO_2-3Cz) and P(NH_2-3Cz) films on ITO-glass.

The electrochemical behavior of the electrodeposited polymer films was investigated by CV in a monomer-free 0.1 M Bu_4NClO_4/MeCN solution. The quantitative details are summarized in Table 1. The CV diagrams of the polymer films of P(NO_2-3Cz) and P(NH_2-3Cz) are shown in Fig. 5. There are two reversible oxidation redox couples at the half-wave potentials ($E_{1/2}$) of 1.06 and 1.28 V for P(NO_2-3Cz), and half-wave potentials of 1.04 and 1.24 V for P(NH_2-3Cz). The oxidation half-wave potential of the P(NO_2-3Cz) film started to oxidize at a higher potential (E_{onset} = 0.88 V) than P(NH_2-3Cz) (E_{onset} = 0.71 V), attributed to the electronic effects arising from the electron-withdrawing properties of the nitro substituents. The P(NH_2-3Cz) film showed only two redox waves, although three oxidation processes of the polyaniline-alike and biscarbazole moieties were expected (Scheme 4). This might be attributed to the fact that the oxidation wave of the polyaniline-alike structure and the first oxidation wave of biscarbazole unit merged and became undistinguished in the CV diagram. For comparative studies, the CV diagrams of (NO_2-NPC) dimer and P(NH_2-NPC) film in a monomer-free 0.1 M Bu_4NClO_4/MeCN solution were also measured and illustrated in Fig. S9†. In general, the CV behaviour of the P(NH_2-3Cz) film is similar to that of P(NH_2-NPC), with a lower oxidation onset potential. However, the CV diagram of the P(NO_2-3Cz) film is totally different from that of the (NO_2-NPC) dimer. The latter showed a relatively higher oxidation potential and an irreversible CV behaviour. Fig. S10† displays the CV curves of the P(NO_2-3Cz) and

P(NH_2-3Cz) at different scanning rates between 50 and 350 mV s^{-1} in 0.1 M Bu_4NClO_4/MeCN solution. The polymer films exhibited two reversible redox couples, attributed to the radical cation and dication states of biscarbazole, respectively (Scheme 4). In the scan rate dependence experiments for P(NO_2-3Cz) and P(NH_2-3Cz) films, both anodic and cathodic peak current values increase linearly with an increasing scan rate, indicating that the electrochemical processes are reversible and not diffusion limited, and the electroactive polymer is well adhered to the working electrode (ITO glass) surface.

The energy levels of the highest occupied molecular orbital (HOMO) and lowest unoccupied molecular orbital (LUMO) of the corresponding polymers were estimated from the $E_{1/2}^{ox}$ values. Assuming that the HOMO energy level for the ferrocene/ferrocenium (Fc/Fc^+) standard is 4.80 eV with respect to the zero vacuum level, the HOMO levels for P(NO_2-3Cz) and P(NH_2-3Cz) were calculated to be 5.42 and 5.40 eV (relative to the vacuum energy level), respectively. Their LUMO energy levels deduced from the band gap calculated from the optical absorption edge were 2.71 and 2.20 eV, respectively (Table 1). According to the HOMO and LUMO energy levels obtained, the polymers in this study might be used as hole injection and transport materials.

Table 1 Optical and electrochemical properties of the electrosynthesized polymers

Polymers	UV-vis absorption wavelength [a] (nm)		Oxidation potential [b] (V)			E_g [c] (eV)	HOMO [d] (eV)	LUMO [d] (eV)
	λ_{max}	λ_{onset}	E_{onset}	$E_{1/2}^{Ox1}$	$E_{1/2}^{Ox2}$			
P(NO_2-3Cz)	305	458	0.88	1.06	1.28	2.71	5.42	2.71
P(NH_2-3Cz)	304	388	0.71	1.04	1.24	3.20	5.40	2.20

[a] UV-vis absorption maximum and onset wavelengths for the polymer films. [b] Read from the first CV scans, in acetonitrile at a scan rate of 50 mV s^{-1} (versus Ag/AgCl). [c] Optical bandgap calculated from absorption edge of the polymer film: $E_g = 1240/\lambda_{onset}$. [d] The HOMO and LUMO energy levels were calculated from $E_{1/2}^{Ox1}$ values of CV diagrams and were referenced to ferrocene (4.8 eV relative to vacuum energy level; E_{onset} = 0.37 V; $E_{1/2}$ = 0.44 V in acetonitrile). $E_{HOMO} = E_{1/2}^{Ox1} + 4.8 - 0.44$ (eV); $E_{LUMO} = E_{HOMO} - E_g$.

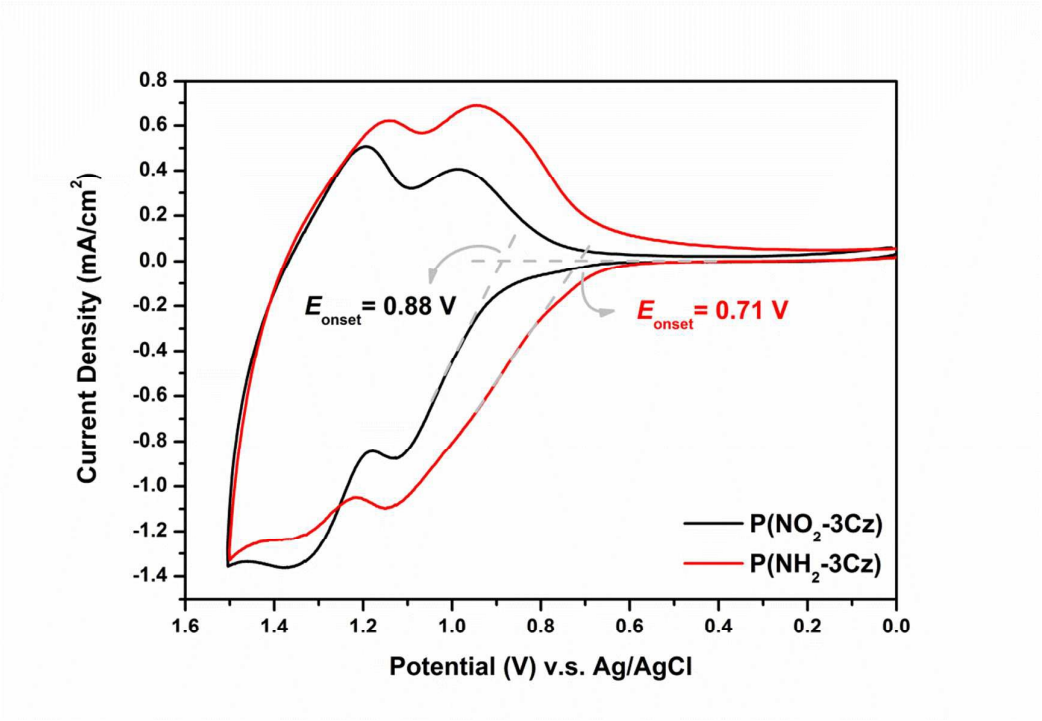

Fig. 5 Cyclic voltammograms of P(NO_2-3Cz) and P(NH_2-3Cz) film on the ITO-coated glass slide in monomer-free 0.1 M Bu_4NClO_4/MeCN solution at a scan rate of 50 mV s^{-1}.

Spectroelectrochemical properties

Spectroelectrochemistry were performed on the electro-generated polymeric films on ITO glass to clarify its electronic structure and optical behavior upon oxidation. The result of polymer P(NO_2-3Cz) film is presented in Fig. 6(a) as the UV-vis-NIR absorbance curves correlated to electrode potentials. In the neutral form, P(NO_2-3Cz) film exhibited strong absorption at wavelength around 304 nm characteristic for π–π* transitions, and it was pale yellow due to some absorption in the region of 400-500 nm. Upon oxidation (increasing applied voltage from 0 to 1.13 V), the absorption of π–π* transition at 304 nm gradually decreased while a new absorption peak at 432 nm and a broadband from about 600 nm extended to the near-IR (NIR) region grew up, which we assigned to the formation of biscarbazole radical cations. The NIR absorption of the polymer can be attributed to the intervalence charge transfer (IVCT) transitions of mixed-valent biscarbazole units or charge-resonance bands in the case of Robin-Day class III systems.[24] When the applied potential was increased to 1.35 V, the absorption at 432 nm decreased gradually accompanied with a broad absorption band at around 710 nm. Meanwhile, they were associated with significant color changes upon oxidation [from pale yellow (L^*: 70;

*a**: 2; *b**: 11) to a deeper yellow (*L**: 60; *a**: 2; *b**: 17) and to blue (*L**: 49; *a**: −5; *b**: 2)] that were homogenous across the ITO glass and easy to detect with the naked eye [Fig. 6(a) inset].

Fig. 6(b) shows the spectral changes of the electro-deposited P(NH_2-3Cz) film upon incremental oxidative scans from 0 to 1.34 V. In the neutral form, the P(NH_2-3Cz) film exhibited strong absorption at λ_{max} of 306 nm and was almost colorless. As the applied voltage was stepped from 0 to 1.14 V, the absorbance at 306 nm decreased, and new peak at 432 nm and a broad absorption band centered at 802 nm gradually increased in intensity. In the same time, the film turned into green (*L**: 56; *a**: 0; *b**: 3). We attribute these spectral changes to the formation of a stable cation radical of biscarbazole unit and polyaniline-alike unit. At a higher applied voltage of 1.34 V, the absorbance at 432 nm decreased and a new broad absorption band at 738 nm, which indicates the formation of dication states. Meanwhile, the film changed color from green to blue (*L**: 50; *a**: −5; *b**: −8). The inset of Fig. 6(b) shows images of the P(NH_2-3Cz) film in uncharged (neutral, colorless), semi-oxidized (green) and fully oxidized states (blue). For comparison, the spectroelectrochemical diagrams of the electrodeposited films of P(NH_2-NPC) and (NO_2-NPC) dimer are included in Fig. S11†. Similar spectral and color changes of the P(NH_2-3Cz) and P(NH_2-NPC) films implies the simultaneous formation of cation radical of biscarbazole unit and polyaniline-alike unit.

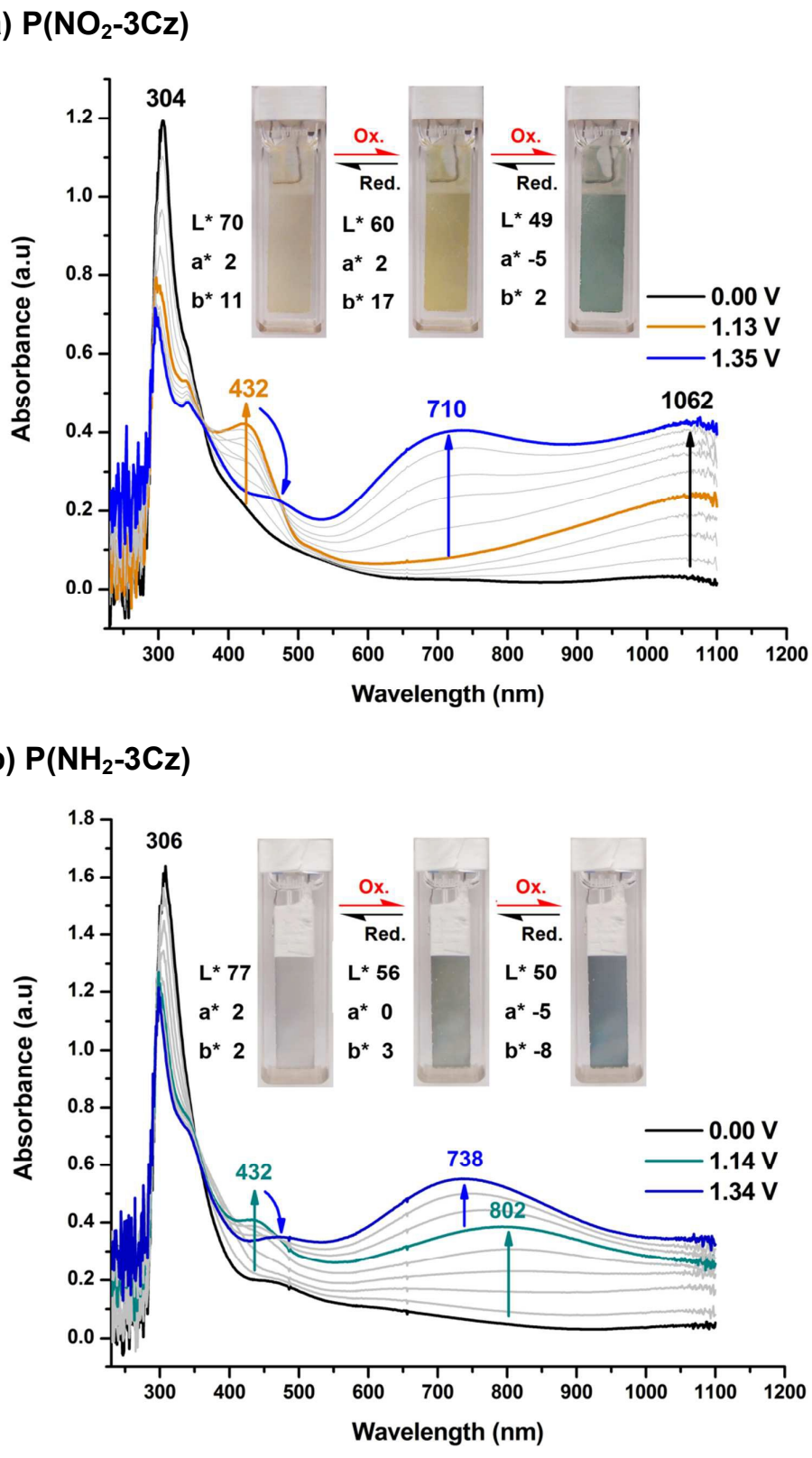

Fig. 6 Spectroelectrograms and color changes of (a) P(NO_2-3Cz) and (b) P(NH_2-3Cz) thin films on ITO-coated glass in 0.1 M Bu_4NClO_4/MeCN at various applied voltages.

Electrochromic switching

Electrochromic switching studies for the P(NO_2-3Cz) and P(NH_2-3Cz) were performed to monitor the percent transmittance changes (Δ%T) as a function of time at their absorption maximum (λ_{max}) and to determine the response time by stepping potential repeatedly between the neutral and oxidized states. The active area of the polymer film on ITO-glass is approximately 1 cm^2. Figs. 7 and 8 depict the optical transmittance of P(NO_2-3Cz) film at 432 and 710 nm as a function of time by applying square-wave potential steps between 0 and 1.22 V and between 0 and 1.38 V with a pulse width of 15 s. The response time was calculated at 90 % of the full-transmittance change, because it is difficult to perceive any further color change with naked eye beyond this point. As shown in Fig. 7(b), P(NO_2-3Cz) attained 90 % of a complete coloring and bleaching in 3.81 and 1.13 s, respectively. The optical contrast measured as Δ%T of P(NO_2-3Cz) between neutral pale yellow and oxidized deeper yellow states was found to be 25 % at 432 nm. The polymer film exhibited a moderate stability in the first ten switching cycles between the neutral and first oxidation states. As the applied voltage was stepped between 0 and 1.38 V, the P(NO_2-3Cz) exhibited an initial Δ%T up to 52 % at 710 nm for the oxidized blue state and required 4.23 s for the coloring step and 1.06 s for the bleaching step. However, the polymer film displayed a larger loss of optical contrast after ten switching cycles between the neutral and the second oxidized states (from 52% to 38%). The electrochromic coloration efficiency (CE; η) can be calculated via optical density using the following equation:

$$\eta = \Delta OD/Q_d$$

where ΔOD is the optical absorbance change, and Q_d (mC/cm^2) is the inject/ejected charge during a redox step. On the basis of this equation, the CE values of P(NO_2-3Cz) were calculated as 62 cm^2/C (at 432 nm) and 35 cm^2/C (at 710 nm).

On the other hand, the switching stability of P(NH_2-3Cz) at λ_{max} = 432 and λ_{max} = 738 were investigated by monitoring the optical contrast (Δ%T) of the thin film upon repeated square-wave potential steps between 0 and 1.22 V with a pulse width of 15 s, and between 0 and 1.41 V with a pulse width of 18 s (see Figs. 9 and 10). In this case, a response time required for 90 % full-transmittance change of 3.74 s for the coloration step and 6.76 s for the bleaching step at 432 nm and 5.51 s for the coloration step and 10.21 s for the bleaching step at 738 nm. In addition, the optical contrast measured as Δ%T recorded at neutral and oxidized forms was found to be 23 % at 432 nm and 43 % at 738 nm. As compared to P(NO_2-3Cz), the P(NH_2-3Cz) film revealed a better electrochromic switching stability possible due to the increased electrochemical stability associated with aniline-alike main chain. As shown in Table 2, the CE values of P(NH_2-3Cz) were calculated as 41 cm^2/C at 432 nm and 48 cm^2/C at 738 nm by chronoamperometry.

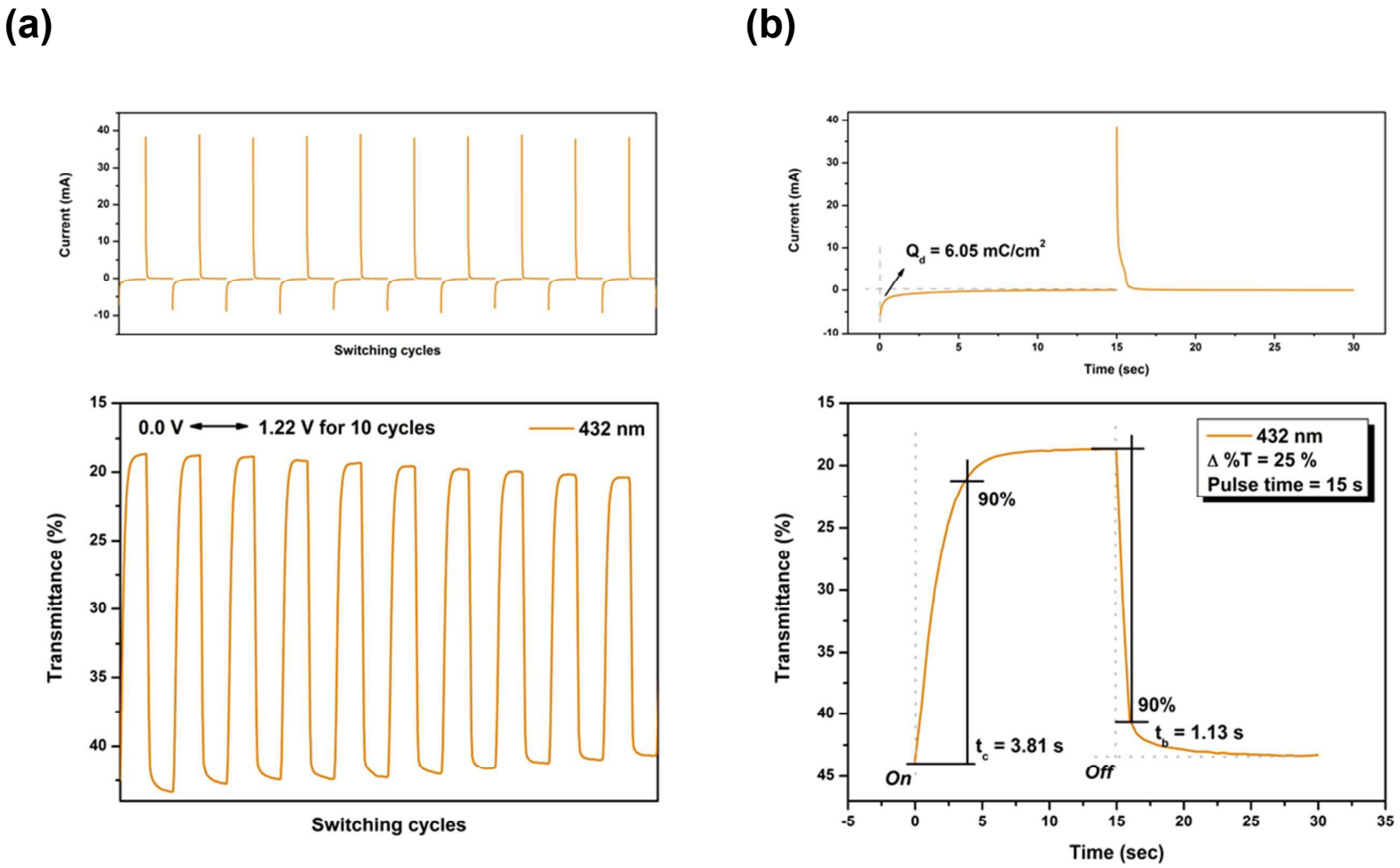

Fig. 7 Potential step absorptiometry of the cast films of P(NO_2-3Cz) on the ITO-glass slide (coated area ~ 1 cm^2) (in MeCN with 0.1 M Bu_4NClO_4 as the supporting electrolyte) by applying a potential step: (a) optical switching at potential 0.00 V ⇔ 1.22 V (10 cycles) with a pulse width of 15 s, monitored at λ_{max} = 432 nm; (b) the 1st cycle transmittance change for the P(NO_2-3Cz) thin film.

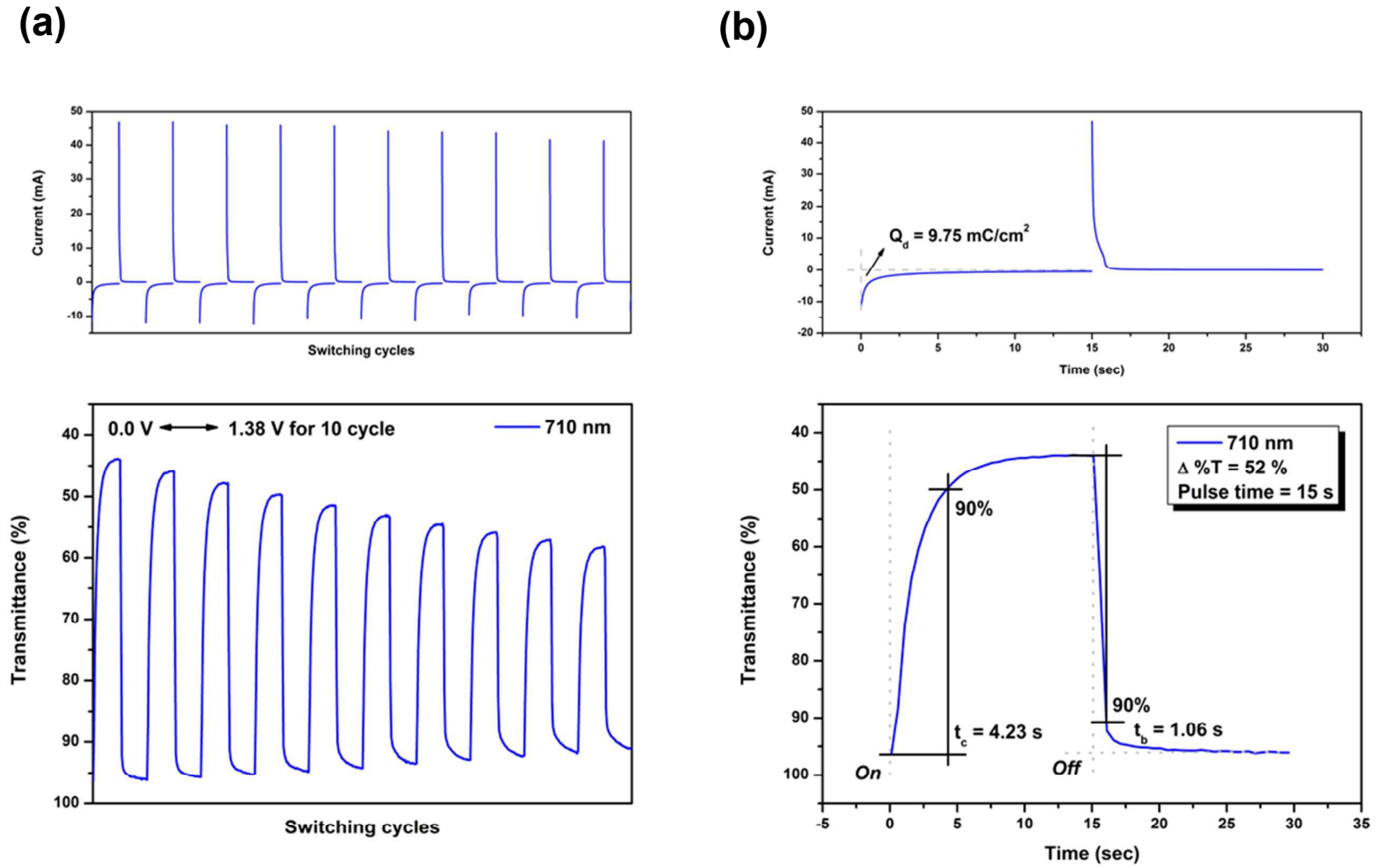

Fig. 8 Potential step absorptiometry of the cast films of P(NO_2-3Cz) on the ITO-glass slide (coated area ~ 1 cm^2) (in MeCN with 0.1 M Bu_4NClO_4 as the supporting electrolyte) by applying a potential step: (a) optical switching at potential 0.00 V ⇔ 1.38 V (10 cycles) with a pulse width of 15 s, monitored at λ_{max} = 710 nm; (b) the 1st cycle transmittance change for the P(NO_2-3Cz) thin film.

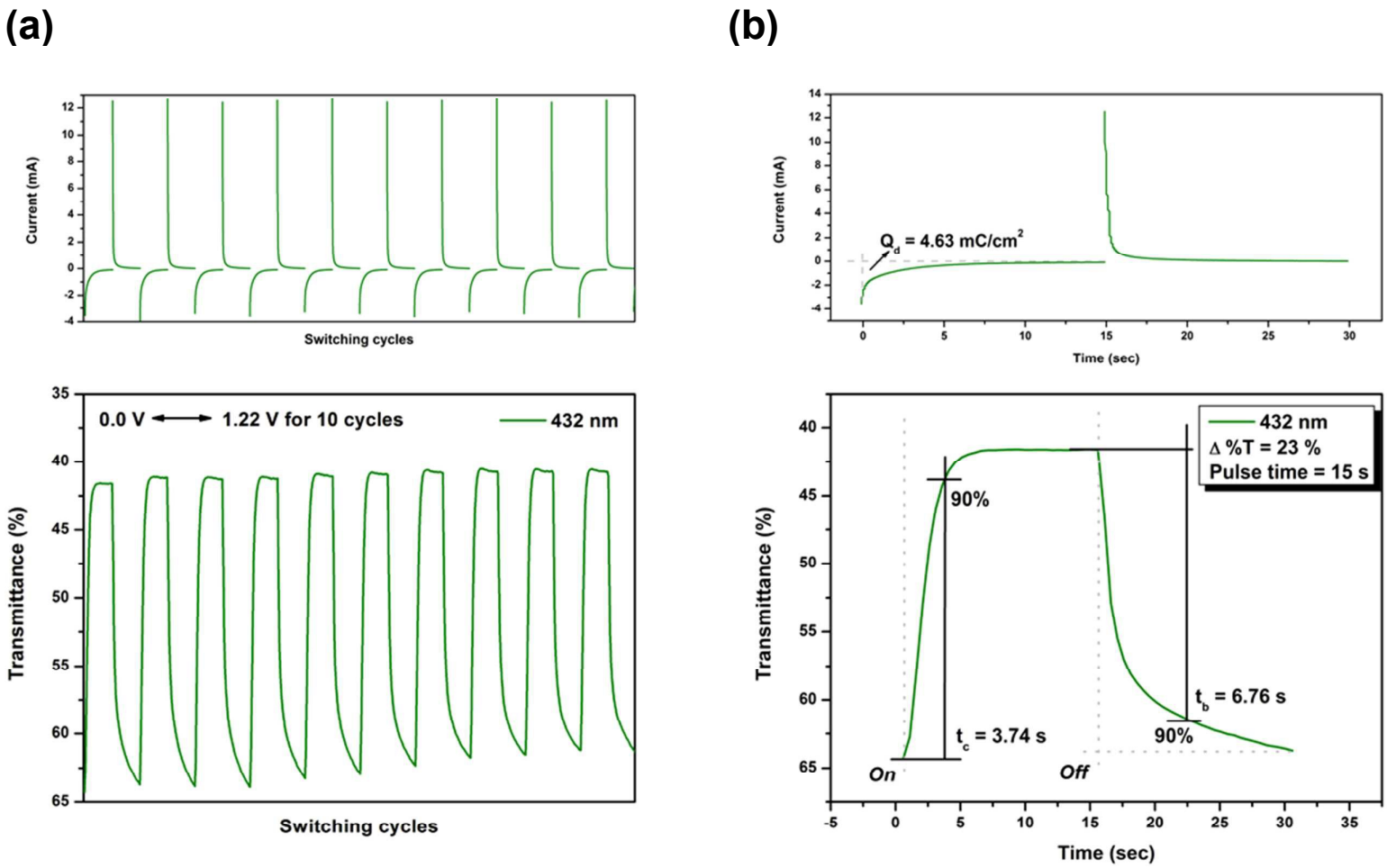

Fig. 9 Potential step absorptiometry of the cast films of P(NH_2-3Cz) on the ITO-glass slide (coated area ~ 1 cm^2) (in MeCN with 0.1 M Bu_4NClO_4 as the supporting electrolyte) by applying a potential step: (a) optical switching at potential 0.00 V ⇔ 1.22 V (10 cycles) with a pulse width of 15 s, monitored at λ_{max} = 432 nm; (b) the 1st cycle transmittance change for the P(NH_2-3Cz) thin film.

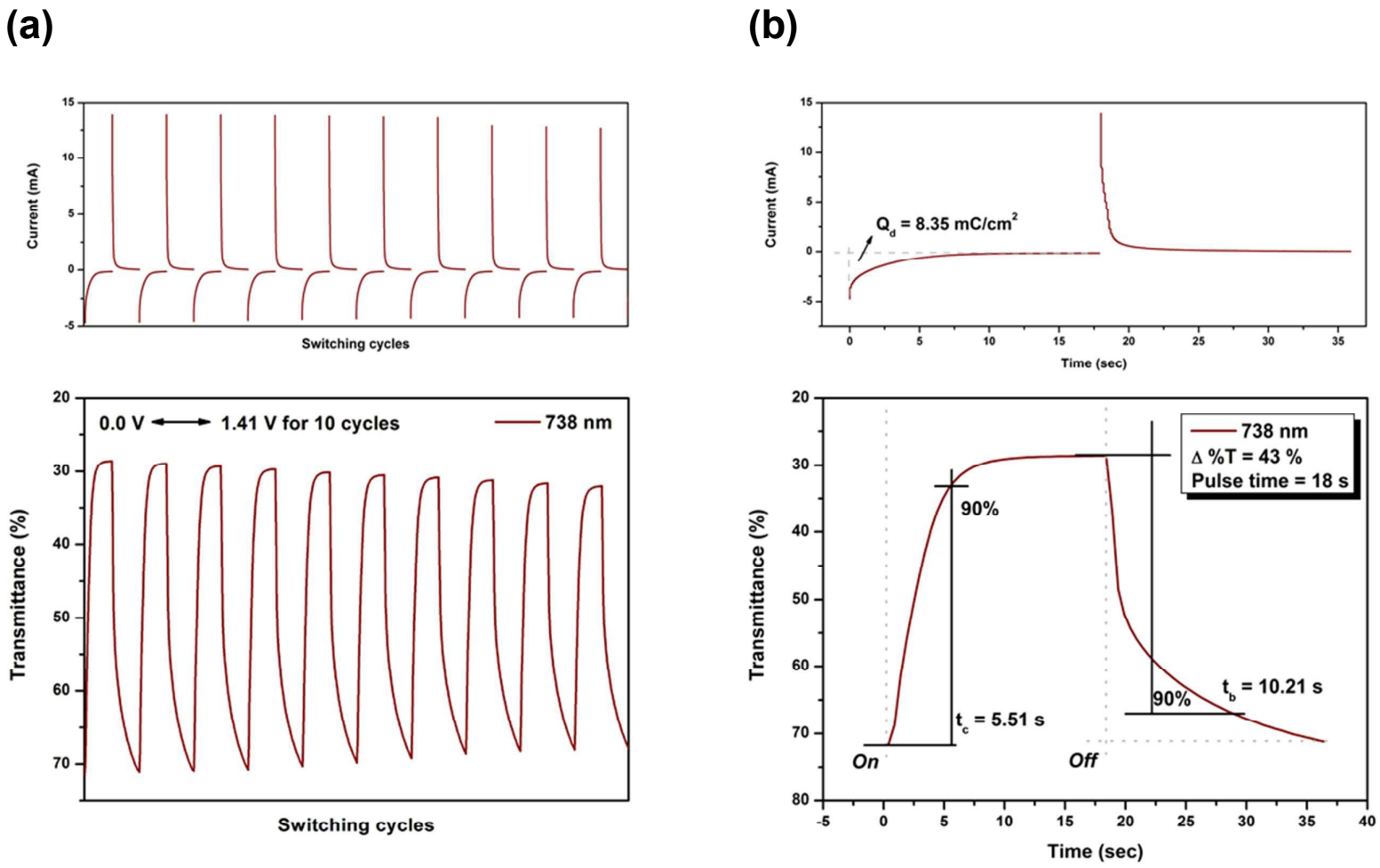

Fig. 10 Potential step absorptiometry of the cast films of P(NH_2-3Cz) on the ITO-glass slide (coated area ~ 1 cm^2) (in MeCN with 0.1 M Bu_4NClO_4 as the supporting electrolyte) by applying a potential step: (a) optical switching at potential 0.00 V ⇔ 1.41 V (10 cycles) with a pulse width of 18 s, monitored at λ_{max} = 738 nm; (b) the 1st cycle transmittance change for the P(NH_2-3Cz) thin film.

Table 2 Electrochromic properties of the polymer films

Polymer	λ_{max}[a] (nm)	Δ%T	Response time[b]		ΔOD[c]	Q_d[d] (mC/cm^2)	CE[e] (cm^2/C)
			t_c (s)	t_b (s)			
$P(NO_2\text{-}3Cz)$	432	25	3.81	1.13	0.375	6.05	62
	710	52	4.23	1.06	0.343	9.75	35
$P(NH_2\text{-}3Cz)$	432	23	3.74	6.67	0.189	4.63	41
	738	43	5.51	10.21	0.404	8.35	48

[a] Wavelength of absorption maximum. [b] Time for 90% of the full-transmittance change. [c] Optical density change (ΔOD) = $\log[T_{bleached} / T_{colored}]$, where $T_{colored}$ and $T_{bleached}$ are the maximum transmittance in the oxidized and neutral states, respectively. [d] Q_d is ejected charge, determined from the in situ experiments. [e] Coloration efficiency (CE) = $\Delta OD/Q_d$.

Electrochromic devices

Based on the foregoing results, it can be concluded that these polymers can be used in the construction of electrochromic devices and optical display. Therefore, single layer electrochromic cells were fabricated as preliminary investigations for the electrochromic applications of these electro-generated polycarbazole films. A schematic illustration of the electrochromic cell is shown in Fig. 11(a). The polymer films were electrodeposited onto ITO-coated glass, thoroughly rinsed, and then dried. Afterwards, the gel electrolyte was spread on the polymer-coated side of the electrode and the electrodes were sandwiched. To prevent leakage, an epoxy resin was applied to seal the device. An electrochromic cell based on $P(NO_2\text{-}3Cz)$ was fabricated which is shown in Fig. 11(b). The $P(NO_2\text{-}3Cz)$ film is pale yellow in the neutral form. When the applied voltage was increased to 2.3 V, the color changed to a deeper yellow. Upon further oxidation at applied potential to 3.0 V, the color changed to blue. When the potential was subsequently set back at 0.0 V, the polymer film turned back to original color. In the other case, the $P(NH_2\text{-}3Cz)$ film is colorless in the neutral form. When voltage was applied (from 0.0 to 2.2 V and 2.4 V), the color changed to yellow green and blue (Fig. 11(c)).

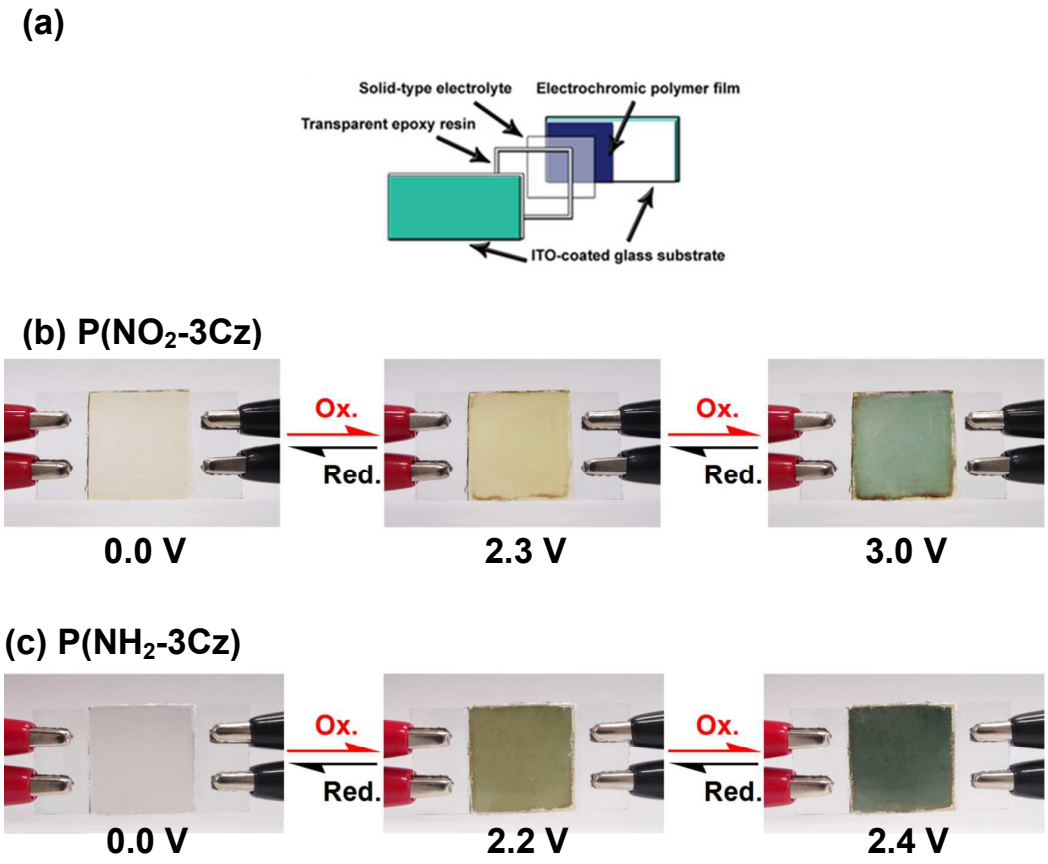

Fig. 11 (a) Schematic illustration of the structure of the electrochromic devices. (b) and (c) Photos of the sandwich-type ITO-coated glass electrochromic cell, using P(NO_2-3Cz) and P(NH_2-3Cz) as active layer.

Conclusions

A series of *N*-phenylcarbazole (NPC) derivatives with different substituents on the *para* position of the *N*-phenyl group have been synthesized and characterized for their electrochemical properties. The oxidized forms of NPC, CN-NPC, COOH-NPC, and NO_2-NPC underwent dimerization to the corresponding biscarbazoles, whereas NH_2-NPC could undergo electrochemical polymerization to form polymer thin film on the electrode surface via the electropolymerization mechanism likely similar to that of polyaniline. 3,6-Bis(*N*-carbazolyl)-substituted NPCs (NO_2-3Cz and NH_2-3Cz) could be readily electropolymerized into polymer films on the electrode surface in an electrolyte solution via the oxidative coupling reactions. The resulting polymer film of P(NO_2-3Cz) exhibited two reversible oxidation redox couples due to oxidations of the biscarbazole unit, and the P(NH_2-3Cz) film showed multistep redox processes attributed to oxidations of the biscarbazole and amino-carbazole moieties. Both of the electro-generated polymer films exhibited obvious color changes during the oxidation

processes. The P(NH_2-3Cz) film showed a slightly lower onset oxidation potential and higher electrochromic stability than the P(NO_2-3Cz) film due to the presence of polyaniline-alike structure. The electro-generated polymer films could be promising materials for electrochromic applications.

Acknowledgement

The authors thank the financial support from the Ministry of Science and Technology of Taiwan, ROC.

References

1 (*a*) D. R. Rosseinsky and R. J. Mortimer, *Adv. Mater.* 2001, **13**, 783−793; (*b*) P. M. S. Monk, R. J. Mortimer and D. R. Rosseinsky, *Electrochromism and Electrochromic Devices*, Cambridge University Press, Cambridge, UK, 2007.

2 (*a*) R. D. Rauh, *Electrochim. Acta*, 1999, **44**, 3165−3176; (*b*) R. Baetens, B. P. Jelle and A. Gustavsen, *Sol. Energy Mater. Sol. Cells,* 2010**, 94**, 87−105.

3 G. Sonmez and H. B. Sonmez, *J. Mater. Chem.,* 2006, **16**, 2473−2477.

4 (*a*) R. J. Mortimer, A. L. Dyer and J. R. Reynolds, *Displays,* 2006**, 27**, 2−18; (*b*) P. M. Beaujuge, S. Ellinger and J. R. Reynolds, *Nat. Mater*., 2008, **7**, 795−799.

5 S. Beaupre, A.-C. Breton, J. Dumas and M. Leclerc, *Chem. Mater*., 2009, **21**, 1504−1513.

6 www.gentex.com

7 (*a*) W. C. Dautremont-Smith, T *Displays,* 1982, **3**, 3−20; (*b*) W. C. Dautremont-Smith, *Displays,* 1982, **3**, 67−80; (*c*) C. G. Granqvist, E. Avendano and A. Azens, *Thin Solid Film,* 2003, 442, 201−211; (*d*) S. Y. Park, J. M. Lee, C. H. Noh and S. U. Son, *J. Mater. Chem.,* 2009, **19**, 7959−964; (*e*) D. T. Gillapie, R. C. Tenent and A. C. Dillon, *J. Mater. Chem.,* 2010, **20**, 9585−9592.

8 (*a*) S. Bernhard, J. I. Goldsmith, K. Takada and H. D. Abruna, *Inorg. Chem.,* 2003, **42**, 4389−4393; (*b*) F. S. Han, M. Higuchi and D. G. Kurth, *Adv. Mater.,* 2007, **19**, 3928−3931; (*c*) F. S. Ham, M. Higuchi and D. G. Kurth, *J. Am. Chem. Soc.,* 2008, **130**, 2073−2081; (*d*) A. Maier, A. R. Rabindranath and B. Tieke, *Adv. Mater.,* 2009, **21**, 959−963; (*e*) A. Maier, H. Fakhrnabavi, A. R. Rabindranath and B. Tieke, *J. Mater. Chem.,* 2011, **21**, 5795−5804.

9 (*a*) R. J. Mortimer, *Electrochim. Acta*, 1999, **44**, 2971−2981; (*b*) P. R. Somani and S. Radhakrishnan, *Mater. Chem. Phys.,* 2002, **77**, 117−133; (*c*) Y. Shirota, *J. Mater. Chem.,* 2000, **10**, 1−25.

10 (*a*) A. A. Argun, P.-H Aubert, B. C. Thompson, I. Schwendeman, C. L. Gaupp, J. Hwang, N. J. Pinto, D. B. Tanner, A. G. MacDiarmid and J. R. Reynolds, *Chem. Mater.,* 2004, **16**, 4401−4412; (*b*) J. Roncali, P. Blanchard and P. Frere, *J. Mater. Chem*., 2005, **15**, 1589−1610; (c) R. M. Walczak and J. R. Reynolds, *Adv. Mater.,* 2006, **18**, 1121–1131; (*d*) R. M. Walczak, J.-H. Jung, J. S. Cowart, Jr. and J. R. Reynolds, *Macromolecules,* 2007, **40**, 7777–7785; (*e*) A. Patra, Y. H. Wijsboom, S. S. Zade, M. Li, Y. Sheynin, G. Leitus and M. Bendikov, *J. Am. Chem. Soc.,* 2008, **130**, 6734−6736; (*f*) A. Patra and M. Bendikov, *J. Mater. Chem*., 2010, **20**, 422−433.

11 (*a*) P. M. Beaujuge and J. R. Reynolds, *Chem. Rev.,* 2010, **110**, 268–320. (*b*) A. Patra, Y. H. Wijsboom, G. Leitus and M. Bendikov, *Chem. Mater*., 2011, **23**, 896–906; (*c*) A. Balan, D. Baran and L. Toppare, *Polym. Chem.,* 2011, **2**, 1029−1043; (*d*) G. Gunbas and L. Toppare, *Chem. Commun*., 2012, **48**, 1083−1101.

12 (*a*) H.-J. Yen, H.-Y. Lin and G.-S. Liou, *Chem. Mater.,* 2011, **23**, 1874−1882; (*b*) H.-J. Yen, H.-Y. Lin and G.-S. Liou, *J. Mater. Chem.,* 2011, **21**, 6230−6237; (*c*) H.-J. Yen and G.-S. Liou, *Polym. Chem.,* 2012, **3**,

255−264; (*d*) H.-J. Yen, C.-J. Chen and G.-S. Liou, *Adv. Funct. Mater.,* 2013, **23**, 5307−5316; (*e)* H.-J. Yen and G.-S. Liou, *Chem. Commun.,* 2013, **49**, 9797−9799.

13 (*a*) Y.-C. Kung and S.-H. Hsiao, *J. Mater. Chem.,* 2010, **20**, 5481−5492; (*b*) Y.-C. Kung and S.-H. Hsiao, *J. Mater. Chem.,* 2011, **21**, 1746−1754; (*c*) S.-H. Hsiao, H.-M. Wang, P.-C. Chang, Y.-R. Kung and T.-M. Lee, *J. Polym. Sci. A: Polym. Chem.,* 2013, **51,** 2925−2938; (*d*) H.-M. Wang and S.-H. Hsiao, *J. Mater. Chem. C*, 2014, **2**, 1553-1564; (*e*) S.-H. Hsiao, H.-M. Wang and S.-H. Liao, *Polym. Chem.,* 2014, **5**, 2473−2483.

14 (*a*) H. Niu, H. Kang, J. Cai, C. Wang, X. Bai and W. Wang, *Polym. Chem*., 2011, **2**, 2804−2817; (*b*) L. Ma, H. Niu, J. Cai, P. Zhao, C. Wang, Y. Lian, X. Bai and W. Wang, *J. Mater. Chem. C*, 2014, **2**, 2272−2282; (*c*) Y. Wang, Y. Liang, J. Zhu, X. Bai, X. Jiang, Q. Zhang and H. Niu, *RSC Adv*., 2015, **5**, 11071−11076.

15 (*a*) J. V. Grazulevicius, P. Strohriegl, J. Pielichowski and K. Pielichowski, *Prog. Polym. Sci.,* 2003, **28**, 1297−1353; (*b*) A. Iraqi and I. Wataru, *Chem. Mater.,* 2004, **16**, 442−448; (*c*) A. Iraqi and I. Wataru, *J. Polym. Sci. A: Polym. Chem.*, 2004, **42**, 6041−6051; (d) H. Yi, A. Iraqi, M. Stevenson, C. J. Elliott and D. G. Lidzey, *Macromol. Rapid Commun*., 2007, **28**, 1155−1160.

16 (*a*) J. Ding, B. Zhang, J. Lu, Z. Xie, L. Wang, X. Jing and F. Wang, *Adv. Mater*., 2009, **21**, 4983−4986; (*b*) C.-C. Lee, M.-k. Leung, P.-Y. Lee, T.-L. Chiu, J.-H. Lee, C. Liu and P.-T. Chou, *Macromolecules,* 2012, **45**, 751−765; (*c*) D. Xia, B. Wang, C. Chen, S. Wang, B. Zhang, J. Ding, L. Wang, X. Jing and F. Wang, *Angew. Chem. Int. Ed.*, 2014, **53**, 1048−1052; (*d*) Y. Wang, S. Wang, N. Zhao, B. Gao, S. Shao, J. Ding, L. Wang, X. Jing and F. Wang, *Polym. Chem*., 2015, **6**, 1180−1191; (*e*) F. Dumur, *Org. Electron*., 2015, **25**, 345−361.

17 (*a*) Y. Pelous, G. Froyer, D. Ades, C. Chevrot and A. Siove, *Polym. Commun*. 1990, **31**, 341; (*b*) J.-F. Morin, M. Leclerc, D. Ades and A. Siove, *Macromol. Rapid Commun*., 2005, **26**, 761−778; (*c*) N. Bloudin and M. Leclerc, *Acc. Chem. Res*., 2008, **41**, 1110−1119; (*d*) P.-L T. Boudreault, S. Beaupre and M. Leclerc, *Polym. Chem.,* 2010, **1**, 127−136.

18 (*a*) J. F. Ambrose and R. F. Nelson, *J. Electrochem. Soc.*, 1968, **115**, 1159−1164; (*b*) J. F. Ambrose, L. L. Carpenter and R. F. Nelson, *J. Electrochem. Soc.,* 1975, **122**, 876−894.

19 (*a*) S. Koyuncu, B. Gultekin, C. Zafer, H. Bilgili, M. Can, S. Demic, I. Kaya and S. Icli, *Electrochim. Acta*, 2009, **54**, 5694–5702; (*b*) B. Wang, J. Zhao, R. Liu, J. Liu and Q. He, *Sol. Energy Mater. Sol. Cells,* 2011**, 95**, 1867–1874; (*c*) O. Usluer, S. Koyuncu, S. Demic and R. A. J. Janssen, *J. Polym. Sci. B: Polym. Phys.,* 2011, **49**, 333−341; (d) C. Xu, J. Zhao, M. Wang, Z Wang, C. Cui, Y. Kong and X. Zhang, *Electrochim. Acta*, 2012, **75**, 28−34.

20 (*a*) Z. Xu, M. Wang, J. Zhao, C. Cui, W. Fan and J. Liu, *Electrochim. Acta,* 2014, **125**, 241−249; (*b*) Z. Xu, M. Wang, W. Fan, J. Zhao and H. Wang, *Electrochim. Acta,* 2015, **160**, 271−280.

21 (*a*) G.-S. Liou, S.-H. Hsiao and H.-W. Chen, *J. Mater. Chem*., 2006, **16**, 1831−1842; (*b*) H.-M. Wang, S.-H. Hsiao, G.-S. Liou and C.-H. Sun, *J. Polym. Sci. A: Polym. Chem.,* 2010, **48**, 4775−4789.

22 (*a*) A. Kulasi, H. Yi and A. Iraqi, *J. Polym. Sci. A: Polym. Chem.*, 2007, **45**, 5957−5967; (*b*) I. Fabre-Francke, M. Zagorska, G. Louarn, P. Hapiot, A. Pron and S. Sadki, *Electrochim. Acta*, 2008, **53**, 6469−6476.

23 S.-K. Chiu, Y.-C. Chung, G.-S. Liou and Y. O. Su, *J. Chin. Chem. Soc*., 2012, **59**, 331−337.

24 (*a*) M. B. Robin and P. Day, *Adv. Inorg. Chem. Radiochem*. 1968, **10**, 247−422; (*b*) C. Lambert and G. Noll, *J. Am. Chem. Soc.,* 1999, **121**, 8434−8442.

Electrochemical synthesis of electrochromic polycarbazole films from *N*-phenyl-3,6-bis(*N*-carbazolyl)carbazoles

Sheng-Huei Hsiao* and Shu-Wei Lin

Department of Chemical Engineering and Biotechnology, National Taipei University of Technology, Taipei 10608, Taiwan. E-mail: shhsiao@ntut.edu.tw

Graphical Abstract

Electroactive and electrochromic polycarbazole films were directly prepared on electrodes from *N*-phenyl-3,6-bis(*N*-carbazolyl)carbazoles by carbazole-based electrochemical oxidative coupling.